Fano-enhanced pulling and pushing optical force on active plasmonic nanoparticles

Dongliang Gao,[1,2] Ran Shi,[1] Yang Huang,[1] and Lei Gao[1,*]

[1]*College of Physics, Optoelectronics and Energy & Collaborative Innovation Center of Suzhou Nano Science and Technology, Soochow University, Suzhou 215006, China*

[2]*Department of Electrical and Computer Engineering, National University of Singapore, 4 Engineering Drive 3, Singapore 117576, Republic of Singapore*

(Received 30 May 2017; published 11 October 2017)

We demonstrate tunable pulling and pushing optical forces on plasmonic nanostructures at plasmon singularity and Fano resonance. The plasmonic nanostructure containing a spherical core with optical gain and a metallic shell shows much larger optical pulling force than a pure gain sphere. When the size of the nanostructure is beyond the quasistatic limit, one can obtain large field enhancement and giant pulling force at the emerged quadrupole mode. The introduction of an optical pump compensates the dissipative loss from the metal shell, thus enabling strong coupling between a narrow quadrupole mode and a board dipole mode, giving rise to Fano resonance. The giant negative forces originate from the reversal of the electric field at Fano resonance, which leads to pulling forces on bound currents and charges. Meanwhile, the separation of the Lorentz force helps to reveal the nature of the pulling forces in the gain system. We have shown that by applying the Lorentz force density formula, it is possible to obtain the correct value of the force inside our complex inhomogeneous structure made up of dispersive and lossy metamaterial irrespective of the electromagnetic momentum density. Our results provide a practical way to manipulate nanoparticles and give deep insight into light-matter interaction.

DOI: 10.1103/PhysRevA.96.043826

I. INTRODUCTION

An object is usually pushed by electromagnetic waves [1] due to the fact that the scattered radiation cannot be unidirectional. In general, the momentum transferred to the object is more than that scattered by the object in the propagation of plane waves. To obtain pulling force, one may reduce the input momentum or increase the forward scattering [1]. Employing optimized multiple plane waves with oblique incidence angle [2] one can reduce the input momentum along the z axis while maximizing the forward scattering. Instead of using multiple plane waves, Chen *et al.* [3] proposed to realize optical pulling force via a Bessel light beam, which can project less photon momentum along the propagation direction and increase the forward scattering by the interference between multipoles of the particle. A proper Bessel beam can pull desired particles along both transverse and longitudinal directions as a tractor beam [4–8], and very recently other types of tractor beams have been demonstrated by using a Gaussian beam [9] or a chiral light [10]. Optical solenoid beams also possess the capability to exert a pulling force on microscopic objects [11]. In addition, light fields with phase gradients [12], optical vortices [13,14], or nonuniform helicity [15] can be exploited for optical manipulation in alternative approaches. These proposed optical beams have promising applications in optical capture, transport, and sorting various objects, such as biological molecules and living cells [16–18]. However, complex beams have their limitations in the amount of control that can be exerted. Due to unintended intensity variations [11] or short working distances [9], objects can be dragged only for several micrometers. In addition, it is still a big challenge to experimentally generate strong nonparaxial Bessel beams or uniform solenoid beams.

While it is usually considered impossible to attract particles with a uniform electromagnetic plane wave, linear momentum of light can be amplified and shows a pulling force when scattered from a lower refractive index medium into a higher one or passing through an object with gain [19,20]. For an active system due to the momentum conservation, a tiny negative optical force is exerted on the stimulated gain medium that scatters extra momentum in the forward direction. However, it is difficult to stably manipulate particles with small optical forces because of their susceptibility to Brownian motion [21]. Enhanced optical forces were found on nanoparticles at the localized surface plasmon resonance [22,23]. Hence, similar effects are expected at gain-assisted surface resonances and plasmon singularities. Meanwhile, plasmonic nanostructures are good candidates to sustain various plasmon resonances [24]. The interaction between resonances in a nanoscale plasmonic system may give rise to Fano resonances, which were observed in both symmetric [25,26] and asymmetric [27] nanostructures. Due to their unique inherent sensitivity, Fano resonances have promising potential applications in ultrafast switches and chemical sensors [28], all-optical light modulation [29], and sorting nanoparticles [30–32].

In this paper, we report enhanced optical pulling and pushing forces on an active plasmonic nanosphere around the Fano resonance. The active nanostructure is composed of an active core and a metallic shell. This type of plasmonic lasing nanostructure also features a low plasmonic lasing threshold [33]. When a uniform plane wave is incident upon the coated nanoparticle, the pulling force can be much larger than that exerted on a single active sphere [19] due to the field enhancement in the nanostructure. By tuning the volume fraction of the gain core, the subradiant quadrupole mode can be redshifted to couple with the superradiant dipole mode, giving rise to Fano resonances. Remarkably, the pulling force can be enhanced by two orders of magnitude due to the strong field enhancement and the dominant negative

*leigao@suda.edu.cn

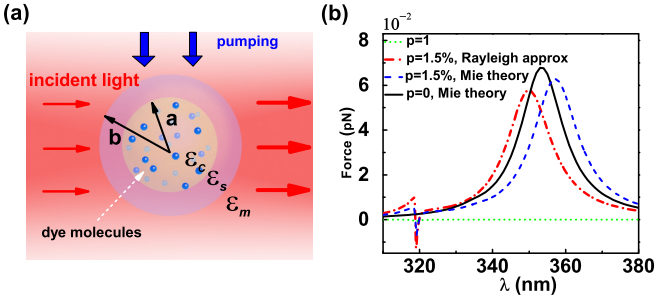

FIG. 1. (a) Schematics of the core-shell nanosphere in vacuum with plane wave incident from left. The core is made of gain material by encapsulating fluorescent dye molecules (small blue particles) into the dielectric material. (b) The normalized forces on gain sphere ($p = 1$), Ag sphere ($p = 0$), and coated active sphere with $p = 1.5\%$. Parameters are $b = 20$ nm and the pump rate is $\Gamma_{\text{pump}} = 1.5\times10^9\ \text{s}^{-1}$. In all the calculations, the intensity of incident light is normalized to $1\ \text{mW}\ \mu\text{m}^{-2}$.

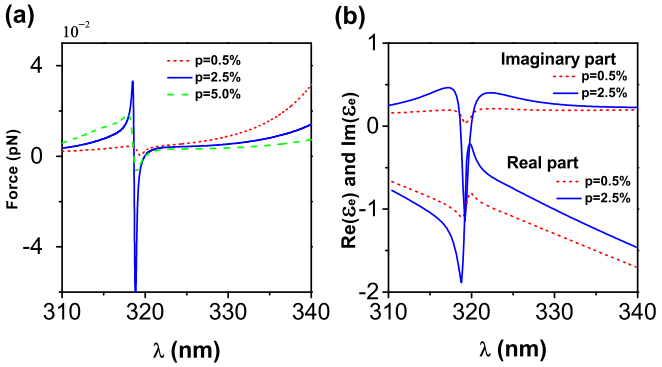

FIG. 2. (a) Optical forces and (b) corresponding equivalent permittivities of the coated particles as a function of incident wavelength. For Rayleigh particles, the enhancement and sign transition of the optical forces can be explained in view of the particle's equivalent permittivity.

Lorentz force on bound currents and charges at the Fano resonance.

II. RESULTS AND DISCUSSION

We consider a core-shell nanosphere with an active (gain) core and a subwavelength plasmonic (metallic) shell, surrounded by a homogeneous medium [see Fig. 1(a)]. The relative permittivity of the metallic shell (Ag) is described by the modified Drude model [34]. The corresponding parameters for the Ag shell are $\varepsilon_\infty = 5.0$, bulk plasma frequency $\omega_p = 9.5\,\text{eV}$, and the reciprocal electron relaxation time for bulk $\Gamma_b = 0.076\,\text{eV}$.The gain effect of the sphere core can be realized by semiconductor material or dye molecules with external pumping [35]. In this paper, we model the gain material as a four-level atomic system, such as fluorescent dye molecules [36,37],

$$\varepsilon_g = \varepsilon_r + \frac{\sigma_a}{\omega^2 + i\Delta\omega_e\omega - \omega_e^2}\frac{(\tau_{21}-\tau_{10})\Gamma_{\text{pump}}}{1+(\tau_{32}+\tau_{21}+\tau_{10})\Gamma_{\text{pump}}}\frac{N_0}{\varepsilon_0}, \tag{1}$$

where $\varepsilon_r = 2.05$ is the relative permittivity of the dielectric host medium, $\sigma_a = 1.71\times10^{-7}\,\text{C}^2/\text{kg}$ is the coupling strength of the polarization density to the electric field, τ_{ij} is the lifetime of the transition from state i to the lower state j, with $\tau_{21} = 3.99$ ns, $\tau_{32} = \tau_{10} = 100$ fs. The center emission angular frequency is $\omega_e = 2\pi c/\lambda_e$, with angular frequency linewidth $\Delta\omega_e = 2\pi c\Delta\lambda_e/\lambda_e^2$. We assume a high concentration for the density of dye molecules as $N_0 = 8\times10^{18}\,\text{cm}^{-3}$ and the pumping rate $\Gamma_{\text{pump}} = 1.5\times10^9\ \text{s}^{-1}$.

Firstly, we consider the small coated nanoparticle in the Rayleigh range, where the incident wavelength is much larger than the dimension of the coated particles. For a nonmagnetic Rayleigh nanoparticle, the time-averaged optical force is written as [19]

$$\langle\mathbf{F}\rangle = \tfrac{1}{2}\mathbf{k}E_{\text{in}}^2\text{Im}(\alpha), \tag{2}$$

where the wave vector $\mathbf{k} = k\mathbf{e_z} = 2\pi\sqrt{\varepsilon_m}/\lambda_0\mathbf{e_z}$ (ε_m is the relative permittivity of the host medium), E_{in} is the electric field amplitude of the incident plane wave, and α is the electric polarizability including the radiation correction [38],

$$\alpha = \alpha_e \Big/ \left(1 - i\frac{2}{3}\frac{k^3\alpha_e}{4\pi\varepsilon_0\varepsilon_m}\right), \tag{3}$$

where α_e is the approximate static polarizability of the core-shell nanoparticle [39],

$$\alpha_e = 4\pi\varepsilon_0\varepsilon_m b^3\frac{(\varepsilon_s-\varepsilon_m)(\varepsilon_c+2\varepsilon_s)+p(\varepsilon_c-\varepsilon_s)(\varepsilon_m+2\varepsilon_s)}{(\varepsilon_s+2\varepsilon_m)(\varepsilon_c+2\varepsilon_s)+2p(\varepsilon_s-\varepsilon_m)(\varepsilon_c-\varepsilon_s)}, \tag{4}$$

with the volume fraction $p = a^3/b^3$. In addition, ε_c and ε_s are the relative permittivities of the core and the shell.

According to Eq. (2), we calculate the optical force in the direction of wave propagation acting on the coated particle by a uniform plane wave $\mathbf{E_{in}} = E_0e^{ikz}e^{-i\omega t}\hat{e}_x$. For simplicity, the background medium is assumed to be air, and we shall use low-power incident light so that the thermal effect on the particle can be neglected. As shown in Fig. 1(b), for coated nanospheres, two resonant peaks for the pushing forces are found at $\lambda_+ = 318$ nm (bonding plasmon resonance) and $\lambda_- = 350$ nm (antibonding plasmon resonance) due to the interaction between the sphere and cavity dipole modes, and the long-wavelength resonant peak exhibits a redshift in comparison with that for the single Ag sphere ($p = 0$). All those can be understood within the hybridization model for nanoshell structures [40]. It should be noted that the large optical pulling force arises between the bonding plasmon resonance and antibonding plasmon resonance, and the pulling force can be about 70 times larger than that of a pure dielectric gain sphere ($p = 1$). To verify the approximate theory, we also perform numerical calculations with full-wave Mie theory and good agreement is found around the range in which pulling force appears.

In Fig. 2(a), the optical force is plotted as a function of the incident wavelength for various volume fractions p. For small volume fractions ($p < 0.5\%$), no pulling force exists in the studied wavelength region. The particle can generate more power in the core with the increase of volume fraction. When the generated power overcomes the scattering forward force, the particle undergoes a pulling force [19]. For $p = 2.5\%$, one achieves the maximal negative force near

$\lambda_- \approx 318$ nm. After that, the optical force decreases with the increases of the core's volume fraction. The high sensitivity of optical force on volume fraction is due to inherent sensitivity of Fano resonance, which is induced by the interaction of bonding plasmon and antibonding plasmon [41]. Small changes in the structure or material of core-shell particles will lead to dramatic variation in optical force. Hence, one could optimize the core-shell particle's structure parameters or external pumping to realize optical manipulation. To understand the enhancement and sign transition of optical forces, we check the corresponding equivalent permittivity $\varepsilon_e \equiv \varepsilon_s[\varepsilon_c(1+2p)+2\varepsilon_s(1-p)]/[\varepsilon_c(1-p)+\varepsilon_s(2+p)]$ of the active coated nanoparticle, as shown in Fig. 2(b). It is evident that the maximal negative force results from the surface plasmon resonance and the plasmon singularity. In the Rayleigh limit (ignoring the radiation correction), we we approximate the optical force as

$$\langle \mathbf{F} \rangle = \frac{3}{2}\mathbf{k}E_0^2 \frac{\varepsilon''}{(\varepsilon'+2)^2+\varepsilon''^2}, \tag{5}$$

with $\varepsilon_e/\varepsilon_m = \varepsilon' + i\varepsilon''$. The optical force is expected to be enhanced at the surface plasmon resonant condition $\varepsilon' = -2$. For metallic material, the resonance shape is broadened by its loss $\varepsilon'' > 0$. However, by introducing the gain in the particle, the loss may be reduced or even overcome. Then at plasmon resonance, the effective loss of a coated nanoparticle is either quite small ($\varepsilon'' \to 0$) or becomes an equivalent gain medium with $\varepsilon'' < 0$, which can exhibit large pushing force or pulling force at the plasmon singularity, respectively. Additionally, we also investigate the roles of nonlocal effects for small particles (not shown in the figures), and find that nonlocality only slightly reduces the field enhancement and blueshifts the resonance frequencies, and the value of optical forces on core-shell spheres is robust to spatial dispersion.

For larger particles, higher-order eigenmodes (such as quadrupole and octupole) arise and interfere with the dipole modes [28]. In this situation, the dipole approximation is not accurate anymore. Precise calculations of optical forces for large spheres can be performed by using Maxwell's stress tensor (MST) $\hat{T} = 1/2(\varepsilon_0\varepsilon_m \mathbf{EE} + \mu_0\mu_m \mathbf{HH}) - 1/4(\varepsilon_0\varepsilon_m|\mathbf{E}|^2 + \mu_0\mu_m|\mathbf{H}|^2)\hat{I}$, where $\mathbf{E}$ and $\mathbf{H}$ are the total fields obtained by Mie theory. Then the time-averaged force on the nanoparticle is the integration over any surface σ surrounding the total coated particle [4,42],

$$\langle \mathbf{F} \rangle = \int_\sigma \langle \hat{T} \cdot \mathbf{n} \rangle ds \tag{6}$$

where $\mathbf{n}$ is the normal outwards direction to the surface σ.

As is shown in Fig. 3(a), a large particle has similar results to a small one, except that additional resonances arise from higher-order modes (such as quadrupole modes at about $\lambda = 457$ nm). The plasmon response of this core-shell nanostructure can be easily understood by the hybridization model [43]. The hybridization between a dipolar sphere and shell plasmons gives rise to a superradiant plasmon mode and a subradiant plasmon mode. Usually the quadrupole mode is suppressed due to the significant optical losses from metal shell. However, the dissipative optical loss can be compensated or even overcome by introducing gain materials into the system [44]. Once the structure becomes nondissipative or weakly dissipative, anomalous light scattering may arise around quadrupole resonance with a narrow and giant line shape [45]. The narrow quadrupole mode interferes constructively and destructively with the broad dipole mode, giving rise to Fano resonance. As is shown in Fig. 3(a), the optical forces are increased with the increase of optical pumping at the Fano resonance, and even flip its direction when the pumping rate reaches the threshold $\Gamma_{\text{pump}} = 0.8\times10^9\ \text{s}^{-1}$. The E fields are greatly enhanced at the surface of the sphere and show the typical quadrupole pattern. Huge excited energies are transferred to the surface plasmon and radiate out like a "lasing spaser" [33,46]. When the generation of power in the core-shell particle is larger than that of scattering from the particle, the light amplification by gain particles leads to the pulling force [19]. Note that the maximal pulling force is about two orders larger than that of a single gain particle. In Fig. 3(b), the Poynting vector lines clearly show that energy flow radiates from the gain structure. Two vortices are formed at the backward side of the particle (represented by yellow lines) due to the strong interaction of the radiated and incident waves. Around the vortices, the streamlines rotate up or down from the xz plane. This counterdirection propagation cancels most of the field momentum [47] in the backward direction. In contrast, radiation in the forward direction (white lines) is emitted without the appearance of vortices, which is in favor of increasing forward linear field momentum and hence realizing large pulling forces.

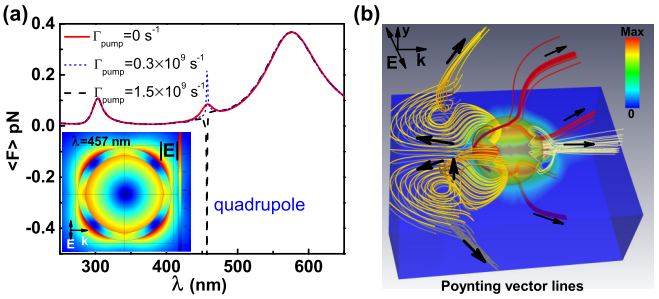

FIG. 3. (a) Optical forces on large particles with $a = 50$ nm and $b = 60$ nm. Insets are the electric field distributions when the particles are under pulling force. (b) Three-dimensional distributions of the Poynting vector's magnitude and Poynting vector lines when the pulling force reaches its maximal value at $\lambda = 457$ nm. The streamlines demonstrate the trajectory of some representative Poynting distribution showing the emitted energy flow from the particle. The black arrows show the direction of the Poynting vectors.

Although far-field scattering of the objects could shed some information on the optical force [1], it is hard to explain quantitatively the origin of the pulling force. Besides, stimulated emission of radiation in the gain system can be overwhelmingly larger than the scattering intensity. The direction of total force has little correlation with the far-field scattering. Compared to the above MST method by the application of the momentum conservation theorem, it is more fundamental to calculate the radiation pressure on an object directly using the Lorentz force [48]. The momentum contributions can be separated into forces on bound currents and charges ($\mathbf{F}_b$) and on free currents ($\mathbf{F}_c$) [49]. In this paper, we only consider nonmagnetic materials, so the bound current density from the magnetization $\nabla \times \mathbf{M}$ and the magnetic charge

density $-\nabla \cdot \mathbf{M}$ are zero. Then the two parts of the Lorentz force density $\mathbf{f}_b$ and $\mathbf{f}_c$ can be reduced as follows [49],

$$\begin{aligned} \mathbf{f}_b &= \tfrac{1}{2}\mathrm{Re}[\varepsilon_0(\nabla \cdot \mathbf{E})\mathbf{E}^* - i\omega\varepsilon_0(\varepsilon_R - 1)\mathbf{E}\times\mathbf{B}^*], \\ \mathbf{f}_c &= \tfrac{1}{2}\mathrm{Re}[\omega\varepsilon_I \mathrm{E}\times\mathrm{B}^*], \end{aligned} \tag{7}$$

where * represents the complex conjugate of a quantity and ε_R (ε_I) is the real (imaginary) part of the relative permittivity in the core or shell. The first and second terms of $\mathbf{f}_b$ are the force contributions from bound electric charges and bound electric currents, respectively. The total Lorentz force on the core-shell nanostructure is the sum of the integration of $\mathbf{f}_b$ and $\mathbf{f}_c$ over the whole structure. In the following, we use the finite element method (COMSOL MULTIPHYSICS V.5.0) to obtain the Lorentz force and verify the results from Mie theory by the MST method.

In a lossy system, the force density on the bound electric charges and currents $\mathbf{f}_b$ can be positive or negative depending on the polarization $\mathbf{P}$ at that position. The force density on free currents $\mathbf{f}_c$ is a pushing force because the incident light attenuates and transfers momentum to free currents in the lossy media [50]. However, in a gain medium the light is magnified and produces extra momentum to the free currents, resulting in negative $\mathbf{f}_c$. When the magnitude of $\mathbf{F}_c$ is larger than $\mathbf{F}_b$, the total force will become a pulling force and drag the particle towards the light source. This also explains why there is a threshold gain for a gain sphere to be pulled by a plane wave [19]. If the particle has the same real part of the permittivity as the background media, there will be no bound electric charge or current at the boundary. Then f_c disappears and the threshold gain vanishes as well.

Core-shell nanostructures have the advantage of low-threshold pumping in realizing plasmon stimulated emissions. Dipole surface plasmon modes in the metallic shell can be excited in this core-shell nanostructure enhancing the electric field in the gain core [33]. However, with the increase of pumping rate, the metallic losses from the shell are compensated around the quadrupole resonance, making the strength of the quadrupole mode comparable to that of the dipole mode. Then the narrow, dark quadrupole mode will couple with the broad, bright dipole mode, giving rise to a Fano resonance. As is shown in Fig. 4, the induced bound force $\mathbf{F}_b$ is dominant, while the force on free currents is basically negligible. When the pumping rate is increased, the field intensity is greatly increased around Fano resonance. However, the enhancement of optical force does not come from the force on free currents in the gain core (the force on free currents of the core remains the same), but from the large force $\mathbf{f}_b$ on the metal shell. This is easy to understand: The bound current density $\mathbf{J}_b = \partial\mathbf{P}/\partial t = -i\omega\varepsilon_0(\varepsilon - 1)\mathbf{E}$ is increased with the enhanced E field. Large $\mathbf{f}_b$ corresponds to a large local polarization density.

Further increasing the pumping rate, the quadrupole mode and dipole mode will interact destructively above Fano resonance. More interestingly, the optical force on core-shell particles will not only be greatly enhanced, but also reverse its direction around Fano resonance. By tuning the pumping rate, one could switch the pulling force and pushing force on active plasmonic nanoparticles. Similar to the pulling-pushing effect on a tapered fiber by photophoretic force [51], external

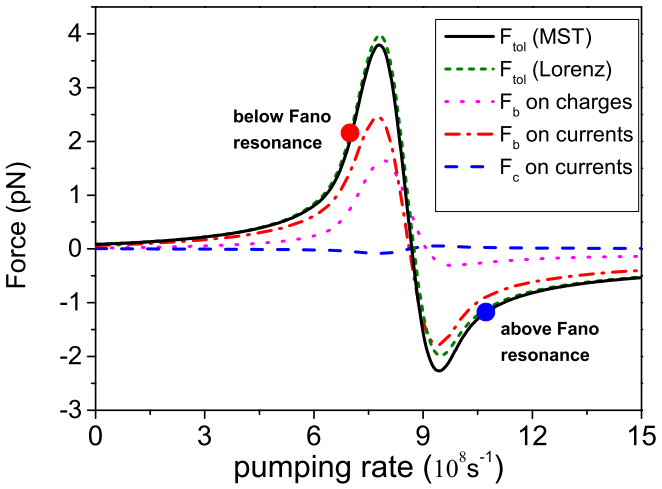

FIG. 4. Forces on a core-shell nanostructure ($a = 50\,\mathrm{nm}$ and $b = 60\,\mathrm{nm}$) for different pumping rates. The total Lorentz forces are divided into two parts: F_b and F_c, respectively. The results from the Lorentz force show good consistency with the results from the MST method. The observable divergence may be due to the vast spatial variation of Lorentz force density when the field intensities are greatly enhanced.

pumping may provide an alternative way to transport nanoparticles back and forth. The interference of two radiative modes generates a very complex near-field distribution, presenting optical vortices of energy flow $\mathbf{E}\times\mathbf{H}^*$ inside the nanoparticle [45]. The handedness of the optical vortex is reversed due to the change of interaction ways from constructive to destructive. From Eq. (7), one can see that the magnitude and direction of energy flow can alter the force density on induced currents, and

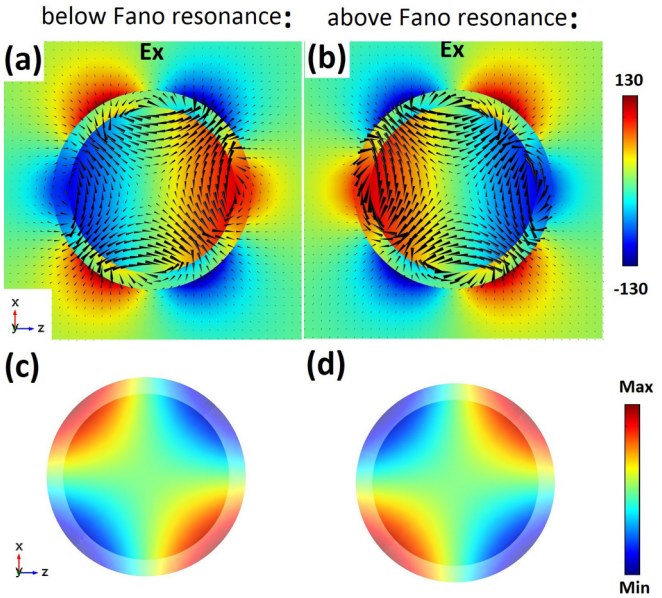

FIG. 5. The distributions of Ex (a,b) and charge density (c,d) at the surfaces of core-shell particles around Fano resonances. The below-Fano resonances ($\Gamma_{\mathrm{pump}} = 0.7\times10^9\,\mathrm{s}^{-1}$) and above-Fano resonances ($\Gamma_{\mathrm{pump}} = 1.1\times10^9\,\mathrm{s}^{-1}$) correspond to the resonances in Fig. 4. The arrows represent the direction of induced current.

therefore change the direction of total force. Figure 5 shows the induced charge distribution and current distribution below Fano resonance and above Fano resonance, respectively. Both induced bound charges at the core-shell surfaces and induced current inside the particle flip around Fano resonance, leading to the reversal of $\mathbf{f}_b$.

III. CONCLUSION

In conclusion, large optical forces are demonstrated on both small and larger nanostructure particles with gain. Pulling and pushing optical force can be switched in different plasmonic modes by controlling the incident wavelength. Large enhancements of negative optical force are achieved at the plasmon singularity and Fano resonance. The giant negative force mainly roots in the Lorentz force on bound currents and charges of the metallic shell. Note that the numbers of dye molecules in the core are estimated to be sufficient to have random distribution of gain elements [46]. One could optimize the parameters such as the concentration of dye molecules, the external pumping, and the volume fraction to realize optical manipulation. Our work may give deep insight into the mechanism of pulling force in gain systems and offer an effective way to obtain large negative forces for nanomanipulation.

ACKNOWLEDGMENTS

This work was supported by the National Natural Science Foundation of China (Grants No. 11374223, No. 11774252, and No. 11504252), the National Science of Jiangsu Province (Grant No. BK20161210), Natural Science Foundation for the Youth of Jiangsu Province (Grant No. BK20150306), the Qing Lan project, "333" project (Grant No. BRA2015353), Natural Science Foundation for Colleges and Universities in Jiangsu Province of China (Grant No. 15KJB140008), and PAPD of Jiangsu Higher Education Institutions.

[1] J. J. Sáenz, Nat. Photon. **5**, 514 (2011).
[2] S. Sukhov and A. Dogariu, Phys. Rev. Lett. **107**, 203602 (2011).
[3] J. Chen, J. Ng, Z. F. Lin, and C. T. Chan, Nat. Photon. **5**, 531 (2011).
[4] A. Novitsky, C.-W. Qiu, and H. Wang, Phys. Rev. Lett. **107**, 203601 (2011).
[5] J. M. Auñón, C. W. Qiu, and M. Nieto-Vesperinas, Phys. Rev. A **88**, 043817 (2013).
[6] A. Novitsky and C.-W. Qiu, Phys. Rev. A **90**, 053815 (2014).
[7] H. Chen, N. Wang, W. Lu, S. Liu, and Z. Lin, Phys. Rev. A **90**, 043850 (2014).
[8] K. Ding, J. Ng, L. Zhou, and C. T. Chan, Phys. Rev. A **89**, 063825 (2014).
[9] O. Brzobohatý, V. Karásek, M. Šiler, L. Chvátal, T. Čižmár, and P. Zemánek, Nat. Photon. **7**, 123 (2013).
[10] D. E. Fernandes and M. G. Silveirinha, Phys. Rev. A **91**, 061801 (2015).
[11] S. H. Lee, Y. Roichman, and D. G. Grier, Opt. Express **18**, 6988 (2010).
[12] Y. Roichman, B. Sun, Y. Roichman, J. Amato-Grill, and D. G. Grier, Phys. Rev. Lett. **100**, 013602 (2008).
[13] J. E. Curtis and D. G. Grier, Phys. Rev. Lett. **90**, 133901 (2003).
[14] J. Ng, Z. F. Lin, and C. T. Chan, Phys. Rev. Lett. **104**, 103601 (2010).
[15] S. Albaladejo, M. I. Marqués, M. Laroche, and J. J. Sáenz, Phys. Rev. Lett. **102**, 113602 (2009).
[16] Y. Zhao, A. A. E. Saleh, and J. A. Dionne, ACS Photon. **3**, 304 (2016).
[17] L. Jauffred, S. M. Taheri, R. Schmitt, H. Linke, and L. B. Oddershede, Nano Lett. **15**, 4713 (2015).
[18] M. Righini, P. Ghenuche, S. Cherukulappurath, V. Myroshnychenko, F. J. Garcia de Abajo, and R. Quidant, Nano Lett. **9**, 3387 (2009).
[19] A. Mizrahi and Y. Fainman, Opt. Lett. **35**, 3405 (2010).
[20] K. J. Webb and Shivanand, Phys. Rev. E **84**, 057602 (2011).
[21] M.-T. Wei and A. Chiou, Opt. Express **13**, 5798 (2005).
[22] H. Xu and M. Käll, Phys. Rev. Lett. **89**, 246802 (2002).
[23] A. S. Zelenina, R. Quidant, and M. Nieto-Vesperinas, Opt. Lett. **32**, 1156 (2007).
[24] L. Zhang, X. Dou, C. Min, Y. Zhang, L. Du, Z. Xie, J. Shen, Y. Zeng, and X. Yuan, Nanoscale **8**, 9756 (2016).
[25] H. Chen, L. Shao, Y. C. Man, C. Zhao, J. Wang, and B. Yang, Small **8**, 1503 (2012).
[26] J. B. Lassiter, H. Sobhani, M. W. Knight, W. S. Mielczarek, P. Nordlander, and N. J. Halas, Nano Lett. **12**, 1058 (2012).
[27] J. Zhang and A. Zayats, Opt. Express **21**, 8426 (2013).
[28] B. Luk'yanchuk, N. I. Zheludev, S. A. Maier, N. J. Halas, P. Nordlander, H. Giessen, and C. T. Chong, Nat. Mater. **9**, 707 (2010).
[29] Y. Yang, W. Wang, A. Boulesbaa, I. I. Kravchenko, D. P. Briggs, A. Puretzky, D. Geohegan, and J. Valentine, Nano Lett. **15**, 7388 (2015).
[30] Z. Li, S. Zhang, L. Tong, P. Wang, B. Dong, and H. Xu, ACS Nano **8**, 701 (2014).
[31] H. J. Chen, S. Y. Liu, J. Zi, and Z. F. Lin, ACS Nano **9**, 1926 (2015).
[32] T. Cao, L. B. Mao, D. L. Gao, W. Q. Ding, and C.-W. Qiu, Nanoscale **8**, 5657 (2016).
[33] J. Pan, Z. Chen, J. Chen, P. Zhan, C. J. Tang, and Z. L. Wang, Opt. Lett. **37**, 1181 (2012).
[34] N. K. Grady, N. J. Halas, and P. Nordlander, Chem. Phys. Lett. **399**, 167 (2004).
[35] G. Strangi, A. De Luca, S. Ravaine, M. Ferrie, and R. Bartolino, Appl. Phys. Lett. **98**, 251912 (2011).
[36] S. Campione, M. Albani, and F. Capolino, Opt. Mater. Express **1**, 1077 (2011).
[37] A. Fang, Z. Huang, T. Koschny, and C. M. Soukoulis, Opt. Express **19**, 12688 (2011).
[38] M. Nieto-Vesperinas, J. J. Sáenz, R. Gómez-Medina, and L. Chantada, Opt. Express **18**, 11428 (2010).
[39] Y. Zeng, Q. Wu, and D. H. Werner, Opt. Lett. **35**, 1431 (2010).
[40] E. Prodan, C. Radloff, N. J. Halas, and P. Nordlander, Science **302**, 419 (2003).
[41] C. Argyropoulos, P. Y. Chen, F. Monticone, G. D'Aguanno, and A. Alu, Phys. Rev. Lett. **108**, 263905 (2012).

[42] A. Novitsky, C.-W. Qiu, and A. Lavrinenko, Phys. Rev. Lett. **109**, 023902 (2012).
[43] E. Prodan and P. Nordlander, J. Chem. Phys. **120**, 5444 (2004).
[44] S. Wuestner, A. Pusch, K. L. Tsakmakidis, J. M. Hamm, and O. Hess, Phys. Rev. Lett. **105**, 127401 (2010).
[45] M. I. Tribelsky and B. S. Luk'yanchuk, Phys. Rev. Lett. **97**, 263902 (2006).
[46] M. A. Noginov, G. Zhu, A. M. Belgrave, R. Bakker, V. M. Shalaev, E. E. Narimanov, S. Stout, E. Herz, T. Suteewong, and U. Wiesner, Nature **460**, 1110 (2009).
[47] D. Gao, A. Novitsky, T. Zhang, F. C. Cheong, L. Gao, C. T. Lim, B. Luk'yanchuk, and C.-W. Qiu, Laser Photon. Rev. **9**, 75 (2015).
[48] B. A. Kemp, T. M. Grzegorczyk, and J. A. Kong, J. Electromagn. Waves Appl. **20**, 827 (2006).
[49] B. A. Kemp, T. M. Grzegorczyk, and J. A. Kong, Phys. Rev. Lett. **97**, 133902 (2006).
[50] B. A. Kemp, J. A. Kong, and T. M. Grzegorczyk, Phys. Rev. A **75**, 053810 (2007).
[51] J. Lu, H. Yang, L. Zhou, Y. Yang, S. Luo, Q. Li, and M. Qiu, Phys. Rev. Lett. **118**, 043601 (2017).